Earth and Planetary Science Letters 454 (2016) 46–54

Contents lists available at ScienceDirect

Earth and Planetary Science Letters

www.elsevier.com/locate/epsl

Emergence of anomalous transport in stressed rough fractures

Peter K. Kang [a,b], Stephen Brown [c], Ruben Juanes [a,c,*]

[a] Dept. of Civil and Environmental Engineering, Massachusetts Institute of Technology, 77 Massachusetts Avenue, Cambridge, MA, USA
[b] Center for Water Resource Cycle Research, Korea Institute of Science and Technology, Seoul, South Korea
[c] Dept. of Earth, Atmospheric and Planetary Sciences, Massachusetts Institute of Technology, 77 Massachusetts Avenue, Cambridge, MA, USA

ARTICLE INFO

Article history:
Received 12 April 2016
Received in revised form 23 August 2016
Accepted 26 August 2016
Available online 6 September 2016
Editor: M. Bickle

Keywords:
groundwater flow
anomalous transport
fracture
roughness
spatial Markov model

ABSTRACT

We report the emergence of anomalous (non-Fickian) transport through a rough-walled fracture as a result of increasing normal stress on the fracture. We show that the origin of this anomalous transport behavior can be traced to the emergence of a heterogeneous flow field dominated by preferential channels and stagnation zones, as a result of the larger number of contacts in a highly stressed fracture. We show that the velocity distribution determines the late-time scaling of particle spreading, and velocity correlation determines the magnitude of spreading and the transition time from the initial ballistic regime to the asymptotic anomalous behavior. We also propose a spatial Markov model that reproduces the transport behavior at the scale of the entire fracture with only three physical parameters. Our results point to a heretofore unrecognized link between geomechanics and particle transport in fractured media.

1. Introduction

Fluid flow and tracer transport through geologic fractures play a critical role in many subsurface processes, including groundwater contamination and remediation, nuclear waste disposal, hydrocarbon recovery, geothermal energy extraction, hydraulic fracturing, and induced seismicity (Bear et al., 1993; Moreno and Neretnieks, 1993; Bodvarsson et al., 1999; Pruess, 2006; Yasuhara et al., 2006). It has been shown—with theoretical and numerical models, as well as with laboratory and field experiments—that macroscopic transport through fracture networks is often *anomalous* (Berkowitz and Scher, 1997; Geiger et al., 2010; Kang et al., 2011b, 2011a, 2015b), characterized by heavy-tailed particle distribution density, both in space and time, and nonlinear temporal evolution of particle mean square displacement (MSD) (Shlesinger, 1974; Bouchaud and Georges, 1990; Metzler and Klafter, 2000).

It is well known that matrix diffusion can induce anomalous transport (Carrera et al., 1998), but our interest here is in rock formations like fractured granite, where the role of matrix diffusion is relatively minor and can often be neglected (Becker and Shapiro, 2000). Geologic fractures, however, are always under significant overburden stress. While confining stress has been shown to impact fluid flow through rough-walled fractures in a fundamental way (e.g. Unger and Mase, 1993; Olsson and Brown, 1993; Pyrak-Nolte and Morris, 2000; Watanabe et al., 2008, 2013; Auradou, 2009; Nemoto et al., 2009; Ishibashi et al., 2015; Pyrak-Nolte and Nolte, 2016), studies of anomalous transport at the scale of individual fractures have so far either ignored the potential role of confining stress (Måløy et al., 1988; Detwiler et al., 2000; Auradou et al., 2001; Bodin et al., 2003a; Drazer et al., 2004; Talon et al., 2012; Wang and Cardenas, 2014), relied on nonmechanistic models (Tsang and Tsang, 1987), or focused on the role of shear stress (Koyama et al., 2008; Vilarrasa et al., 2011; Jing et al., 2013). As a result, the mechanistic underpinning and theoretical modeling for the emergence of anomalous transport in rough fractures under normal stress remains unexplored.

Here, we demonstrate that an increase in the normal stress on a rough fracture can induce anomalous transport. Normal stress transforms the fracture geometry from a relatively homogeneous to a very heterogeneous flow structure: as the mean fracture aperture decreases, the flow organizes into preferential-flow channels and stagnation zones. To study the impact of normal stress on flow and transport, we first generate rough fracture surfaces, solve the nonlocal elastic contact problem on the rough-walled fractures under normal stress, and solve the flow and transport problem through the stressed rough-walled fractures. Then, by quantitatively analyzing the key mechanisms that lead to anomalous transport, we develop a parsimonious model of the transport dynamics—the proposed model can reproduce the transport behavior at the scale of the entire fracture with only three physical

* Corresponding author at: Dept. of Civil and Environmental Engineering, Massachusetts Institute of Technology, 77 Massachusetts Avenue, Cambridge, MA, USA.
E-mail address: juanes@mit.edu (R. Juanes).

http://dx.doi.org/10.1016/j.epsl.2016.08.033
0012-821X/

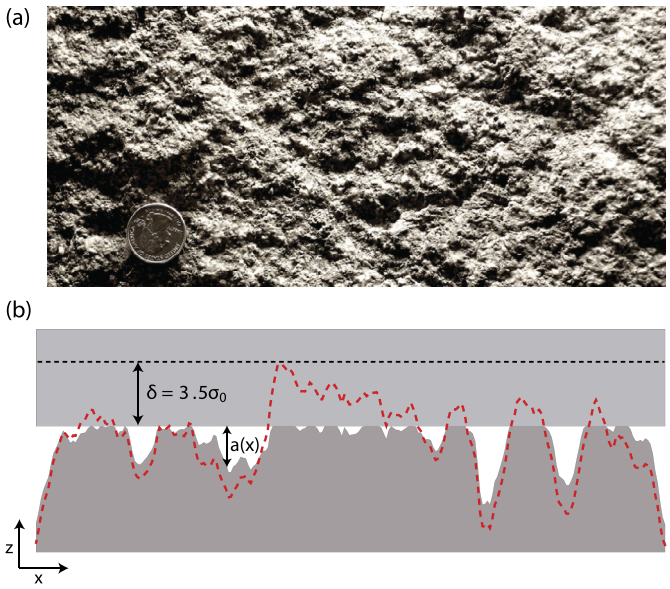

Fig. 1. (a) Grayscale photograph of a rough fracture surface of granite, obtained from an outcrop in Vermont, USA. Self-affine fractal surfaces are known to be good representations of natural fractures. (b) As the normal displacement δ increases, contact areas appear; we solve the nonlocal elastic contact problem to obtain aperture fields. Aperture profiles at $\delta = 0$ and at $\delta = 3.5\sigma_0$ are shown. $\delta = 0$ corresponds to the state when the two surfaces are at first contact (zero normal stress).

parameters. Our findings advance our understanding of transport through fractured media by linking anomalous transport behavior with the geomechanical properties of fractures and their state of stress.

2. Generating rough fracture surfaces

Geologic fractures typically exhibit a complex surface topography [Fig. 1(a)]. Here, we construct realistic rough fracture surfaces using the spectral synthesis method, which captures the fundamental property that fractures are self-affine fractal surfaces (Power and Tullis, 1991). The methodology relies on two key ingredients: a power spectral density function and a phase spectrum (Power and Tullis, 1991; Brown, 1995; Glover et al., 1998). The power spectral density of real fracture surfaces exhibits power-law decay as a function of the wavenumber k (inverse of wavelength λ), where the exponent is determined by the fractal dimension D_f of the fracture surface, and the intercept is determined by the standard deviation of surface heights, σ_f. The phase spectrum, in contrast, is a nearly random process, independent of frequency (white noise).

Experimental observations also indicate that the top and bottom fracture surfaces are strongly correlated for long wavelengths but poorly correlated for short wavelengths (Brown, 1995; Glover et al., 1998). This is physically intuitive: top and bottom surfaces that were once perfectly mated will maintain similar large-scale structures, but small-scale structures will be disturbed during fracturing process. To incorporate this fundamental observation into the synthetic rough surface generator, and to allow for a gradual decay in correlation with wavenumber, we introduce the phase correlation function $\gamma = \frac{1}{2}[1 + \mathrm{erf}(-(k - k_c)/\theta)]$, where θ is a model parameter that determines the rate of correlation decay, and $k_c = 1/\lambda_c$ is the wavenumber at where the phase correlation between the top and bottom surface is 0.5.

Once the power and phase spectra of the top and bottom surfaces have been set, we generate the two surfaces by performing an inverse Fourier transform. The aperture field at first contact ($a_{\delta=0}(x, y)$) can be obtained by substracting top and bottom surfaces heights such that the minimum aperture is zero without deformation; δ is the compressive normal displacement from first contact [Fig. 1(b)]. For the aperture field presented in this study, the mean aperture value at first contact is $\overline{a}_{\delta=0} = 4.3\sigma_0$ where σ_0 is the standard deviation of aperture values at $\delta = 0$. For the results presented in this paper, we choose $D_f = 2.3$, $\theta = 4$, $\lambda_c = L/15$, $\sigma_f = L/100$ where L is the domain size, and digital resolution of 256×256 pixels.

3. Elastic contact problem

We obtain the geometry of the stressed rough fracture by solving an elastic contact problem on the synthetic rough surface subject to normal stress [Fig. 1(b)]. Fractured rock often exhibits elastic behavior, and past studies employed an elastic model to investigate the role of normal stress on rough surfaces (e.g., Bandis et al., 1983; Brown and Scholz, 1985; Hopkins, 1990; Unger and Mase, 1993; Pyrak-Nolte and Morris, 2000; Petrovitch et al., 2014). We employ realistic values of the elastic constants for rock under geologic conditions (Wang, 2000; Pollard and Fletcher, 2005; Johnson and DeGraff, 1988): shear modulus $G = 20$ GPa, and Poisson ratio $\nu = 0.25$, which are in the range of common values for natural rocks such as granite, basalt, limestone and sandstone (Johnson and DeGraff, 1988). We consider the long-range deformation produced by the force at each contact, and the combined effect of multiple contacts (Andrews, 1988; Unger and Mase, 1993). As the distance between the top and bottom surfaces decreases due to an increase in confining stress, a region of interpenetration between the top and bottom surfaces emerges. We constrain the deformation such that there is no interpenetration between the two surfaces. This is a mixed boundary value problem with displacement prescribed over part of the surface and normal stress prescribed over the remainder of the surface. The analytical solution for vertical/normal displacement due to a point force on an elastic half space is known as the Boussinesq solution, $B(r) = \frac{(1-\nu)}{2\pi G}\frac{1}{r}$, where r is the distance from the point force. The normal displacement $w(x, y)$ is obtained by convolution of the Boussinesq solution with the stress field $S(x, y)$: $w(x, y) = \iint S(x', y')B(r)dx'dy'$ (Andrews, 1988; Unger and Mase, 1993). We use the discrete Fourier transform to solve the mixed boundary value problem, which makes the solution periodic.

By solving the elastic deformation problems for increasing values of the normal displacement δ, we obtain aperture maps at different levels of stress. The probability distributions of aperture values at four different displacements ($\delta = 0$, $1.5\sigma_0$, $2.5\sigma_0$, and $3.5\sigma_0$) clearly show a dramatic change in the aperture heterogeneity [Fig. 2(d)]. The aperture distribution is initially Gaussian but becomes heavy tailed as contact areas emerge. A broad aperture distribution implies a broad local (pixel-sale) fracture conductivity, which in turn impacts flow and transport. We note that solving the elastic deformation problem leads to different fracture geometry compared with simply removing the overlaps between the two surfaces, especially at high normal stress.

4. Impact of stress on the flow field

To study the impact of stress on the flow field, we perform a fluid flow simulation for incompressible fluid with constant viscosity and density on the final solution of the elastic deformation simulation at each value of the displacement δ [Fig. 1(b)]. We take the aperture map, $a(x, y)$, as the gap width in an equivalent parallel plate model (Moreno et al., 1988). By applying the lubrication approximation, we obtain a Darcy type equation for the gap-averaged fluid velocity, $\mathbf{u} = -\frac{a^2}{12\eta}\nabla P$, where η is the fluid dynamic viscosity and P is the fluid pressure (Tsang and Tsang, 1987;